

Valence states and spin structure of spinel FeV_2O_4 with different orbital degrees of freedom

J.-S. Kang,* Jihoon Hwang, D. H. Kim, and Eunsook Lee

Department of Physics, The Catholic University of Korea (CUK), Bucheon 420-743, Korea

W. C. Kim and C. S. Kim

Department of Physics, Kookmin University, Seoul 136-702, Korea

Sangil Kwon and Soonchil Lee

Department of Physics, KAIST, Daejeon 305-701, Korea

J.-Y. Kim

Pohang Accelerator Laboratory, POSTECH 790-784, Korea

T. Ueno and M. Sawada

Hiroshima Synchrotron Radiation Center (HSRC), Hiroshima University, Higashi-Hiroshima 739-0046, Japan

Bongjae Kim, Beom Hyun Kim, and B. I. Min

Department of Physics, POSTECH, Pohang 790-784, Korea

(Received 17 February 2012; revised manuscript received 9 April 2012; published 23 April 2012)

The electronic structure of spinel FeV_2O_4 , which contains two Jahn-Teller active Fe and V ions, has been investigated by employing soft x-ray absorption spectroscopy (XAS), soft x-ray magnetic circular dichroism (XMCD), and nuclear magnetic resonance (NMR). XAS indicates that V ions are trivalent and Fe ions are nearly divalent. The signs of V and Fe $2p$ XMCD spectra are opposite to each other. It is found that the effect of the V $3d$ spin-orbit interaction on the V $2p$ XMCD spectrum is negligible, indicating that the orbital ordering of V t_{2g} states occurs from the real orbital states and that the orbital moment of a V^{3+} ion is mostly quenched. NMR shows that V spins are canted to have a Yafet-Kittel-type triangular spin configuration.

DOI: [10.1103/PhysRevB.85.165136](https://doi.org/10.1103/PhysRevB.85.165136)

PACS number(s): 75.25.Dk, 78.20.Ls, 71.70.Ej, 76.60.-k

The crystal distortion due to the cooperative Jahn-Teller (JT) effect plays a crucial role in leading to charge ordering (CO) or orbital ordering (OO) in magnetic oxides.¹ Well-known examples are colossal magnetoresistance perovskite manganites, where the doubly degenerate e_g orbitals of Mn $3d$ states give rise to CO and/or OO. Similarly, the partially occupied triply degenerate t_{2g} orbitals induce the OO instability in spinel vanadates of ZnV_2O_4 ²⁻⁴ and MnV_2O_4 ,^{5,6} which have trivalent V^{3+} ($3d^2$) ions in the octahedral (O_h) sites. In the spinels that contain divalent Fe^{2+} ($3d^6$) ions at the tetrahedral (T_d) sites, Fe^{2+} ions tend to induce the JT distortion and the cubic-to-tetragonal phase transition.^{7,8} FeCr_2O_4 , FeV_2O_4 , and FeAl_2O_4 are considered to belong to this category.⁹

In spite of the interesting physics related to the OO in spinel oxides, not much work has been reported yet as to the effect of competition and/or cooperation between the orbital degrees of freedom at different sites. In this aspect, FeV_2O_4 is a good candidate because it has two different magnetic ions at different sites and both of them have the orbital degrees of freedom. Katsufuji *et al.*¹⁰ reported the temperature (T) dependence of high-resolution x-ray diffraction (XRD) and magnetization in FeV_2O_4 . They observed the successive structural phase transitions, accompanied by the change in the magnetic easy axis and the large magnetostriction. FeV_2O_4 undergoes the structural transitions, from cubic to tetragonal, orthorhombic, and tetragonal at ~ 140 , ~ 110 , and ~ 70 K, respectively. Ferrimagnetic ordering occurs simultaneously

with the structural transition at $T \sim 110$ K. They proposed that the competition of Fe^{2+} and V^{3+} orbitals is the origin of the successive structural transitions. Nishihara *et al.*¹¹ reported the detailed investigation of the magnetic properties of FeV_2O_4 . They observed the spin-glass-like transition at ~ 86 K, in addition to the ferrimagnetic transition at $T_c \sim 110$ K. They suggested that the spin structure of FeV_2O_4 at low temperature would have a spiral long-range ordering, similarly as in CoCr_2O_4 .¹² Furthermore, polycrystalline FeV_2O_4 exhibits the magnetic-field-dependent capacitance or polarization behavior, which has attracted attention in relation to multiferroicity.^{8,13}

The unresolved issues in spinel vanadates, such as ZnV_2O_4 , are the nature of the OO state and the size of the orbital moment of V ions.¹⁴⁻¹⁷ One group claimed that the OO arises from the real orbital states and that the orbital moment is small,¹⁴ while the others claimed that the OO arises from the complex orbital states and the orbital moment is as large as $\sim 1.0 \mu_B$.^{15,16} We address the same questions for FeV_2O_4 . In order to clarify the origin of the magnetic and structural properties of FeV_2O_4 , it is essential to understand the electronic and spin structure of FeV_2O_4 first. In this aspect, soft x-ray absorption spectroscopy (XAS)^{18,19} and soft x-ray magnetic circular dichroism (XMCD)^{20,21} are powerful experimental tools for studying the valence and spin states of transition-metal ions in solids and the element-specific local magnetic moments of spin and orbital components, respectively.

In this work, we have investigated the electronic and spin structure of FeV_2O_4 by employing XAS, XMCD, and nuclear magnetic resonance (NMR). We have found that the effect of the V $3d$ spin-orbit (SO) interaction on V $2p$ XMCD is negligible, and that the OO of V ions occurs from the real orbital states of d_{xz} and d_{yz} . V spins are found to be canted from Fe spins, resulting in a Yafet-Kittel-type triangular spin configuration.

Polycrystalline FeV_2O_4 samples were synthesized by using solid-state reaction methods.^{11,22} XRD showed that the samples have the single-phase spinel structure. XAS and XMCD measurements were performed by employing the total electron yield mode at the 2A beamline of Pohang Light Source and also at the BL-14 beamline of the Hiroshima Synchrotron Radiation Center. To remove the surface contamination, samples were cleaned *in situ* by repeated scrapings with a diamond file under a pressure better than 3×10^{-10} Torr. XAS/XMCD data were obtained at $T = 80, 150,$ and 300 K. The photon energy resolution was set at ~ 100 meV at $h\nu \approx 600$ eV. XMCD spectra were obtained under an external magnetic field of 0.6 T and 1.3 T by using the circularly polarized light with the degree of circular polarization $>95\%$. The line shapes were essentially the same. In this paper, we show the data obtained at $T = 80$ K. All the XAS/XMCD spectra were normalized to the incident photon flux. NMR spectra were obtained by using the conventional spin echo method in a T range of 4 – 20 K with a custom-made spectrometer. To estimate the spin canting angle, the resonance frequency was measured for various magnetic fields up to 7 T. ^{51}V NMR signals were searched for between 200 MHz and 350 MHz.

Figure 1(a) shows the Fe $2p$ XAS spectrum of FeV_2O_4 at $T = 80$ K, which is divided into the SO split L_3 ($2p_{3/2}$) and L_2 ($2p_{1/2}$) parts. The line shapes of XAS spectra are essentially the same between $80 \text{ K} \leq T \leq 300 \text{ K}$. As a guide of the valence states of Fe ions, it is compared to those of reference Fe oxides, Fe metal, and a similar spinel oxide FeCr_2O_4 . The

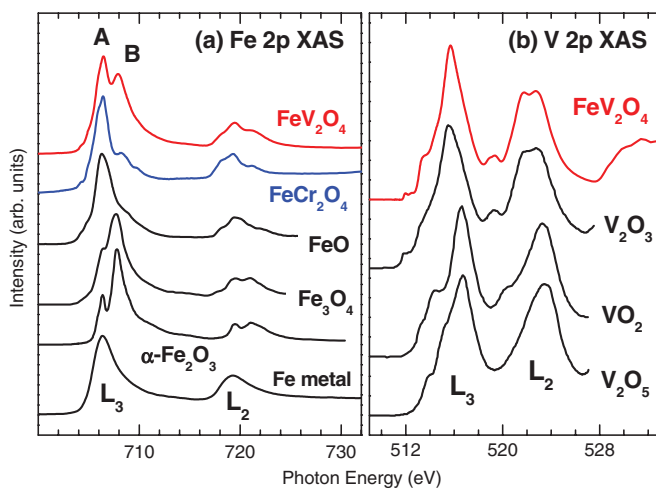


FIG. 1. (Color online) (a) Fe $2p$ XAS spectra of FeV_2O_4 in comparison to those of FeCr_2O_4 (our data), FeO (Ref. 23), $\alpha\text{-Fe}_2\text{O}_3$ (Ref. 23), and Fe_3O_4 (Ref. 23), and Fe metal (our data). (b) V $2p$ XAS spectra of FeV_2O_4 in comparison to those of V_2O_3 (Refs. 24 and 25), VO_2 (Ref. 26), V_2O_5 (Ref. 24). Reference spectra are arbitrarily scaled.

Fe $2p$ XAS spectrum of FeV_2O_4 is qualitatively similar to that of FeCr_2O_4 having the nominal valency of Fe^{2+} . But the higher-energy peak (B) is more pronounced than in FeCr_2O_4 and weaker than in a well-known mixed-valent Fe_3O_4 that has the nominal valency of $\text{Fe}^{2.67+}$. We have roughly estimated the valence states of Fe ions in FeV_2O_4 to be $\nu(\text{Fe}) \sim 2.2$, indicating that the ratio of $\text{Fe}^{3+}/\text{Fe}^{2+}$ is ~ 0.2 .²⁷

Similarly, Fig. 1(b) shows the V $2p$ XAS spectrum of FeV_2O_4 , in comparison to those of reference V oxides. It is observed that the V $2p$ XAS spectrum of FeV_2O_4 is very similar to that of V_2O_3 , but different from those of VO_2 and V_2O_5 in the peak positions and the line shapes, suggesting that V ions are nearly trivalent ($\text{V}^{3+}: 3d^2$) in FeV_2O_4 . This finding is supported by the NMR data, shown in Fig. 4. On the other hand, if FeV_2O_4 is stoichiometric, there should be V^{2+} components because Fe^{3+} components are observed [see Fig. 1(a)]. Note, however, that there are no stoichiometric oxides with V^{2+} states. In fact, according to previous reports,^{8,10} excess Fe ions are often formed in FeV_2O_4 samples so as to become $\text{Fe}[\text{Fe}_x\text{V}_{2-x}]\text{O}_4$. Based on these facts, we interpret that Fe^{3+} components arise in part from the excess Fe ions in $\text{Fe}^{2+}[\text{Fe}_x^{3+}\text{V}_{2-x}^{3+}]\text{O}_4$ with $x \leq 0.2$. The amount of $x \leq 0.2$, found in this study, is consistent with those of the previous reports.^{8,10} This point is discussed further in Fig. 2.

Figure 2 shows the measured XMCD spectra of Fe and V $2p$ states in FeV_2O_4 , obtained at ≈ 80 K. We do not show the XMCD data of $T \geq 150$ K, because XMCD signals become very weak as T is increased from 80 K to 150 K. This feature is consistent with $T_c \sim 110$ K. In contrast to a simple single-peak structure in Fe metal,²¹ the Fe $2p$ XMCD spectrum of FeV_2O_4 exhibits the multiplet structures, reflecting the localized nature of Fe $3d$ electrons in FeV_2O_4 . Note that the Fe $2p$ XMCD peaks are located under the divalent Fe^{2+} XAS peak only, but not under the trivalent Fe^{3+} XAS peak. Therefore we conclude that Fe $2p$ dichroism signals arise from divalent Fe^{2+} ions only. This finding suggests that most of the Fe^{3+} ions do not belong to the intrinsic spinel structure, but belong to the nonmagnetic

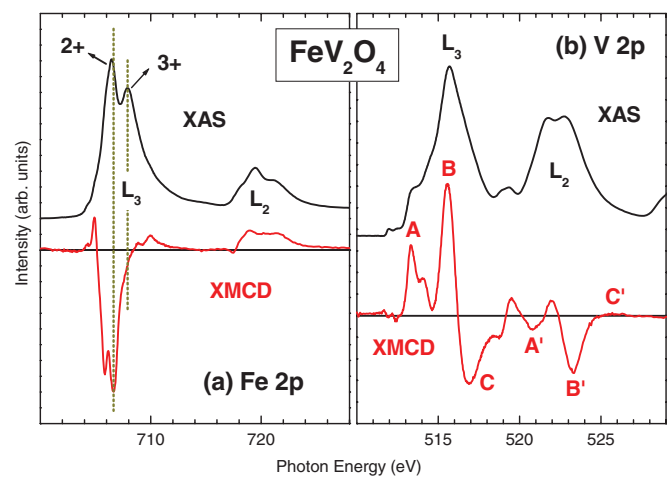


FIG. 2. (Color online) (a) Comparison of Fe $2p$ XMCD and XAS spectra of FeV_2O_4 . In order to help to identify the location of the Fe $2p$ XMCD peaks, the guide lines are added as gray dotted lines. (b) Similarly for V $2p$ states.

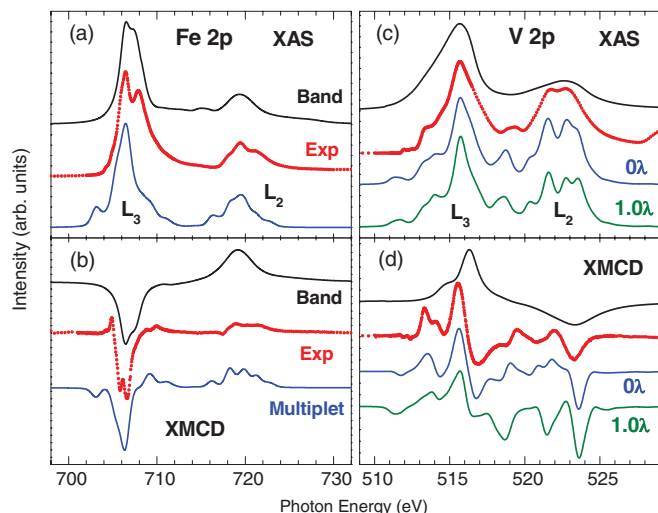


FIG. 3. (Color online) Comparison of the theoretical Fe and V $2p$ XAS and XMCD spectra to the corresponding experimental spectra (red dots). (a), (b) for Fe $2p$ and (c), (d) for V $2p$. Top spectra in each panel (black lines) denote the calculated spectra for low- T tetragonal, obtained from the FLAPW calculation, and the others denote those obtained from the multiplet calculation. For the multiplet calculation for V^{3+} , we show two cases with (1.0 λ) and without (0 λ) the SO effect, for $10Dq = 2.0$ eV.

oxidized phase. In fact, we have found that the surfaces of polycrystalline FeV_2O_4 samples are easily oxidized to produce trivalent Fe^{3+} ions.²⁸

The complicated V $2p$ dichroism signals in Fig. 2(b) originate from the final-state multiplet structures of trivalent V^{3+} ions, as will be shown in Fig. 3(d). Further, it appears complex because the L_3 and L_2 peaks are not well separated due to the small SO splitting in V $2p$ states. Figure 2 reveals that the sign of the major part of the V $2p$ XMCD (>0) is opposite to that of the Fe $2p$ XMCD (<0). Since the different signs in XMCD imply the opposite directions of the corresponding magnetic moments, this finding indicates that the magnetic moments of Fe^{2+} and V^{3+} ions are antiparallel to each other, which is shown more clearly in Fig. 5(a). This finding is consistent with the antiferromagnetic (AFM) coupling between A (T_d) and B (O_h) sites in spinel compounds.

Figure 3 provides calculated XAS and XMCD spectra of Fe and V ions in FeV_2O_4 , by employing both the all-electron FLAPW band method²⁹ and the crystal field multiplet scheme.³⁰ Since XAS and XMCD experiments were performed at $T \lesssim 80$ K, the measured data correspond to those of the orthorhombic or low- T tetragonal structure of FeV_2O_4 .³¹ Indeed, among the band results for different structures, those for low- T tetragonal provide the best agreement with experiment, even though the multiplet peaks in the experimental spectra are not described well. On the other hand, the multiplet calculations for Fe^{2+} and V^{3+} agree well with experiment.³² In the crystal field multiplet calculations for V^{3+} , we have varied both the crystal field parameter $10Dq$, and the Jahn-Teller splitting parameter Δ_{JT} in the D_{4h} symmetry, and found that those with $10Dq = 2.0$ eV and $\Delta_{JT} \approx 0$ eV match well with the experimental spectra. This $10Dq$ value is similar to $10Dq = 2.18$ eV for low- T

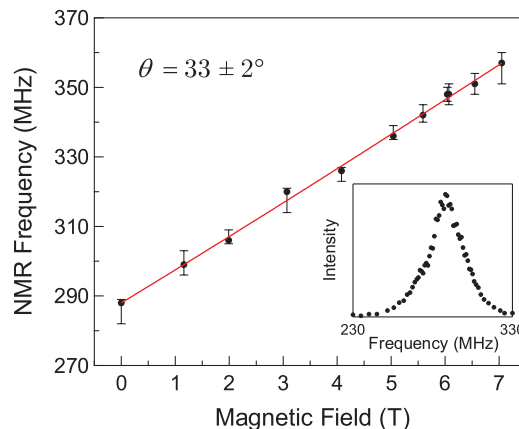


FIG. 4. (Color online) The ^{51}V NMR peak frequency vs magnetic field obtained at 4 K. Inset: The ^{51}V NMR spectrum.

tetragonal, obtained in the band calculation.³³ For given $10Dq$ and Δ_{JT} , we have also varied the SO coupling parameter of the $3d$ states, λ . Interestingly, the spectra with 0λ match best with experiment. This finding suggests that the $3d$ SO coupling plays a minor role in the OO in low- T tetragonal FeV_2O_4 and that the OO of V t_{2g} states occurs from the real orbital states (d_{xz}/d_{yz}),¹⁴ but not from the complex orbital states ($d_{xz} \pm id_{yz}$).¹⁶ Then the orbital moment of a V^{3+} ion would be mostly quenched.

In Fig. 4 is plotted the NMR frequency change with the external magnetic field. The inset shows the ^{51}V NMR spectrum obtained in the zero field at $T = 4$ K. The spectrum shows a well-defined single peak centered around 288 MHz. Since NMR measures the magnetic field that nuclei experience, the NMR resonance frequency for magnetic materials at zero external field is proportional to the magnetic moment of the ion and the hyperfine constant. Note that the ^{51}V NMR resonance frequencies of V_2O_3 ³⁴ and MnV_2O_4 ³⁵ are 208 and 281 MHz, respectively, while the spectra of V^{4+} ions are in the range of 55–80 MHz.^{36,37} Hence the resonance frequency of 288 MHz for FeV_2O_4 indicates that V ions in FeV_2O_4 are mostly in V^{3+} states, which agrees with the findings in XAS and XMCD (Figs. 1 and 2).

In the presence of the external magnetic field, the NMR resonance frequency, $f(H_{ext})$, is determined by the total field that is the vector sum of the hyperfine field, H_{hf} , and the external field, H_{ext} : $f(H_{ext}) = \gamma_N |\vec{H}_{hf} + \vec{H}_{ext}| = \gamma_N \sqrt{H_{hf}^2 + H_{ext}^2 + 2H_{hf}H_{ext} \cos \theta}$, where γ_N is the nuclear gyromagnetic ratio and θ is the angle between H_{hf} and H_{ext} . Since the magnetization axis aligns in parallel with H_{ext} in ferrimagnetic materials such as FeV_2O_4 , θ corresponds to the spin canting angle. θ and H_{hf} can be obtained by tracing the change in $f(H_{ext})$ with H_{ext} . As shown in Fig. 4, $f(H_{ext})$ of the V spectrum increases with increasing H_{ext} . This visually shows that the direction of the magnetic moment of the V ions is antiparallel to H_{ext} because the hyperfine constant of V is negative. The frequency changes almost linearly in the experimental field range, as expected for $H_{ext} \ll H_{hf}$. Fitting the data to the above equation results in $\theta = 33^\circ \pm 2^\circ$ and $H_{hf} = 25.7$ T. The canting of V spin is consistent with the fact that the B - B exchange interaction of V spins is also AFM.

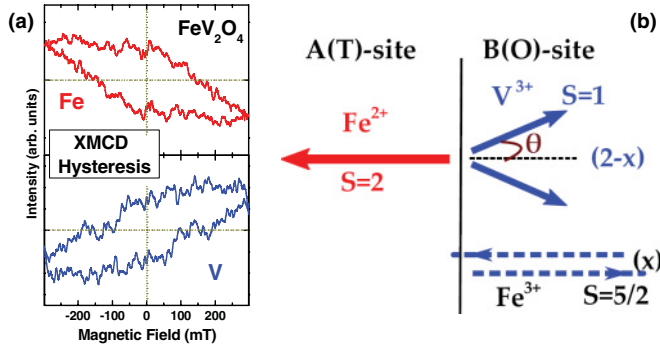


FIG. 5. (Color online) (a) Element-specific hysteresis curves of FeV_2O_4 , derived from Fe and V L_3 XMCD signals at $T = 80$ K, respectively. (b) Schematic spin structure of FeV_2O_4 at $T = 0$ K. The red and blue solid-line arrows represent major spins in A (T_d) and B (O_h) sites, respectively, while the dotted arrows represent Fe^{3+} spins.

Figure 5(a) shows the element-specific hysteresis curves of FeV_2O_4 , derived from the XMCD signals by employing the procedure of Refs. 38 and 39. This figure shows clearly that the magnetic moments of Fe^{2+} and V^{3+} ions are antiparallel to each other. Based on the analyses of XAS/XMCD and NMR spectra and theoretical calculations, we provide a schematic drawing of the spin structure of FeV_2O_4 in Fig. 5(b). The essence of our finding is that V spins tend to be canted to have a Yafet-Kittel-type⁴⁰ triangular spin configuration. If one considers the total saturated magnetic moment, $\sim 2.15 \mu_B$, of polycrystalline FeV_2O_4 ,^{8,10,13} and the nominal spin-only magnetic moments of Fe^{2+} ($4 \mu_B$) and V^{3+} ($2 \mu_B$), then the

V spin canting angle θ in Fig. 5(b) would be $\sim 60^\circ$, which is contradictory to $\theta = 33^\circ$ obtained by NMR. This situation is similar to that for MnV_2O_4 .³⁵ On the other hand, $\theta = 33^\circ$ can be compatible with the saturated magnetic moment, if the orbital moment of a V^{3+} ion is very large, i.e., as large as $\sim 0.9 \mu_B$, as in ZnV_2O_4 .^{15,16} However, our finding in V $2p$ XMCD [in Fig. 3(d)] that the orbital moment of a V^{3+} ion is nearly quenched in FeV_2O_4 refutes this scenario. Indeed, according to Ref. 33, the estimated orbital moment of V^{3+} ion in FeV_2O_4 was only $0.1 \mu_B$, which is too small to produce $\theta = 33^\circ$. In order to solve this discrepancy, neutron scattering experiments would be useful.

In conclusion, we have found that the valence states of Fe and V ions in FeV_2O_4 are mainly divalent and trivalent, respectively. Small Fe^{3+} components are observed, which arise mainly from the nonmagnetic oxidized phase at the surface. XMCD shows that V and Fe spins are opposite to each other. V $2p$ XMCD indicates that the orbital magnetic moment for a V ion is mostly quenched due to the negligibly small spin-orbit interaction in V $3d$ states, and that the orbital ordering of V t_{2g} states occurs from the d_{xz} and d_{yz} real orbital states.⁵¹ V NMR shows that V ions are trivalent and that the canting angle θ of the V^{3+} hyperfine field is $\theta = 33^\circ \pm 2^\circ$.

This work was supported by the NRF under Contracts No. 2011-0022444 and No. 2009-0079947, and in part by the 2011 Research Fund of the CUK. C.S.K. and W.C.K. acknowledge support by NRF 2011-0000323. S.K. and S.L. acknowledge support by NRF 2009-0078342. J.Y.K. acknowledges support by NRF 2009-0088969. The PLS is supported by POSTECH and MEST. Part of this work was done at HSRC under the approval of the Proposal Assessing Committee.

*Corresponding author: kangjs@catholic.ac.kr

¹M. Imada, A. Fujimori, and Y. Tokura, *Rev. Mod. Phys.* **70**, 1039 (1998).

²Y. Ueda, N. Fujiwara, and H. Yasuoka, *J. Phys. Soc. Jpn.* **66**, 778 (1997).

³M. Reehuis, A. Krimmel, N. Büttgen, A. Loidl, and A. Prokofiev, *Eur. Phys. J. B* **35**, 311 (2003).

⁴S.-H. Lee, D. Louca, H. Ueda, S. Park, T. J. Sato, M. Isobe, Y. Ueda, S. Rosenkranz, P. Zschack, J. Iñiguez, Y. Qiu, and R. Osborn, *Phys. Rev. Lett.* **93**, 156407 (2004).

⁵R. Plumier and M. Sougi, *Physica B* **155**, 315 (1989).

⁶T. Suzuki, M. Katsumura, K. Taniguchi, T. Arima, and T. Katsufuji, *Phys. Rev. Lett.* **98**, 127203 (2007).

⁷M. Tanaka, T. Tokoro, and Y. Aiyama, *J. Phys. Soc. Jpn.* **21**, 262 (1966).

⁸Q. Zhang, K. Singh, F. Guillou, C. Simon, Y. Breard, V. Caignaert, and V. Hardy, *Phys. Rev. B* **85**, 054405 (2012).

⁹Even though FeSc_2S_4 has JT-active Fe^{2+} ions, it does not exhibit the cubic-to-tetragonal phase transition. V. Fritsch, J. Hemberger, N. Büttgen, E.-W. Scheidt, H.-A. Krug von Nidda, A. Loidl, and V. Tsurkan, *Phys. Rev. Lett.* **92**, 116401 (2004).

¹⁰T. Katsufuji, T. Suzuki, H. Takei, M. Shingu, K. Kato, K. Osaka, M. Takata, H. Sagayama, and T. Arima, *J. Phys. Soc. Jpn.* **77**, 053708 (2008).

¹¹S. Nishihara, W. Doi, H. Ishibashi, Y. Husokoshi, X.-M. Ren, and S. Mori, *J. Appl. Phys.* **107**, 09A504 (2010).

¹²Y. Yamasaki, S. Miyasaka, Y. Kaneko, J.-P. He, T. Arima, and Y. Tokura, *Phys. Rev. Lett.* **96**, 207204 (2006).

¹³H. Takei, T. Suzuki, and T. Katsufuji, *Appl. Phys. Lett.* **91**, 072506 (2007).

¹⁴Y. Motome and H. Tsunetsugu, *Phys. Rev. B* **70**, 184427 (2004).

¹⁵O. Tchernyshyov, *Phys. Rev. Lett.* **93**, 157206 (2004).

¹⁶T. Maitra and R. Valenti, *Phys. Rev. Lett.* **99**, 126401 (2007).

¹⁷V. Hardy, Y. Breard, and C. Martin, *Phys. Rev. B* **78**, 024406 (2008).

¹⁸F. M. F. de Groot, J. C. Fuggle, B. T. Thole, and G. A. Sawatzky, *Phys. Rev. B* **42**, 5459 (1990).

¹⁹G. van der Laan and I. W. Kirkman, *J. Phys.: Condens. Matter* **4**, 4189 (1992).

²⁰B. T. Thole, P. Carra, F. Sette, and G. van der Laan, *Phys. Rev. Lett.* **68**, 1943 (1992).

²¹C. T. Chen, Y. U. Idzerda, H.-J. Lin, N. V. Smith, G. Meigs, E. Chaban, G. H. Ho, E. Pellegrin, and F. Sette, *Phys. Rev. Lett.* **75**, 152 (1995).

²²M. Wakihara, Y. Shimzu, and T. Katsura, *J. Solid State Chem.* **3**, 478 (1971).

²³T. J. Regan, H. Ohldag, C. Stamm, F. Nolting, J. Lüning, J. Stöhr, and R. L. White, *Phys. Rev. B* **64**, 214422 (2001).

- ²⁴M. Abbate, H. Pen, M. T. Czyzyk, F. M. F. de Groot, and J. C. Fuggle, *J. Electron Spectrosc. Relat. Phenom.* **62**, 181 (1993).
- ²⁵C. F. Hague, J.-M. Mariot, V. Ilakovac, R. Delaunay, M. Marsi, M. Sacchi, J.-P. Rueff, and W. Felsch, *Phys. Rev. B* **77**, 045132 (2008).
- ²⁶M. Abbate, F. M. F. de Groot, J. C. Fuggle, Y. J. Ma, C. T. Chen, F. Sette, A. Fujimori, Y. Ueda, and K. Kosuge, *Phys. Rev. B* **43**, 7263 (1991).
- ²⁷We have analyzed the Fe $2p$ XAS spectrum of FeV_2O_4 with the weighted sum of those of FeCr_2O_4 (Fe^{2+}) and $\alpha\text{-Fe}_2\text{O}_3$ (Fe^{3+}).
- ²⁸J. Hwang, D. H. Kim, E. Lee, J.-S. Kang, W. C. Kim, C. S. Kim, S. W. Han, S. C. Hong, B.-G. Park, and J.-Y. Kim, *J. Korean Magn. Soc.* **21**, 198 (2011).
- ²⁹Bongjae Kim and B. I. Min (unpublished).
- ³⁰E. Stavitski and F. M. F. de Groot, *Micron* **41**, 687 (2010).
- ³¹Our sample exhibits a magnetic anomaly near $T \approx 72$ K, which would be related to the transition from the orthorhombic structure to the low- T tetragonal structure.
- ³²Note that the calculated spectra do not describe the higher-energy peak in the Fe L_3 XAS spectrum, which is mainly due to Fe^{3+} ions of the nonmagnetic oxidized phase at the surface.
- ³³S. Sarkar and T. Saha-Dasgupta, *Phys. Rev. B* **84**, 235112 (2011).
- ³⁴H. Yasuoka, K. Motoya, Y. Nakamura, and J. P. Remeika, *AIP Conf. Proc.* **10**, 1411 (1973).
- ³⁵S.-H. Baek, N. J. Curro, K.-Y. Choi, A. P. Reyes, P. L. Kuhns, H. D. Zhou, and C. R. Wiebe, *Phys. Rev. B* **80**, 140406 (2009).
- ³⁶Y. Ueda, K. Kosuge, S. Kachi, H. Yasuoka, H. Nishihara, and A. Heidemann, *J. Phys. Chem. Solids* **39**, 1281 (1978).
- ³⁷M. Itoh, H. Yasuoka, Y. Ueda, and K. Kosuge, *J. Magn. Magn. Mater.* **31**, 343 (1983); **34**, 343 (1983).
- ³⁸E. Goering, A. Fuss, W. Weber, J. Will, and G. Schütz, *J. Appl. Phys.* **88**, 5920 (2000).
- ³⁹M. Sawada, T. Tagashira, K. Furumoto, T. Ueno, A. Kimura, H. Namatame, and M. Taniguchi, *J. Electron Spectrosc. Relat. Phenom.* **184**, 280 (2011).
- ⁴⁰Y. Yafet and C. Kittel, *Phys. Rev.* **87**, 290 (1952).